SOUND FIELD MEASUREMENT AT AN ENCLOSURE OPENING USING REFRACTO-VIBROMETRY

Tong Xiao, Benjamin Halkon, Sebastian Oberst, Shuping Wang and Xiaojun Qiu
Centre for Audio, Acoustics and Vibration, University of Technology Sydney, Australia
e-mail: Tong.Xiao@student.uts.edu.au, Benjamin.Halkon@uts.edu.au

A sound field can be measured by an array of microphones distributed across the area of interest or by moving a smaller number of microphones sequentially. Such procedures can be time-consuming and expensive when high spatial resolution is required. Furthermore, the presence of physical microphones might disturb the sound field. Refracto-vibrometry is based on the acousto-optic effect. It can serve as an alternative method to measure sound pressure at all the points of interest without disturbing the sound field. In this paper, three methods, the filtered back-projection, the truncated singular value decomposition and the Tikhonov regularisation methods, are used to evaluate the sound field at an enclosure opening. Comparison with a microphone array shows that the Tikhonov regularisation method yields the best result.
Keywords: refracto-vibrometry, sound field measurement, laser Doppler vibrometer

1. Introduction

Many sound field control applications require the acoustic pressure field to be measured in advance. This is commonly achieved by an array of microphones distributed across the field or by altering the position of a smaller number of microphones sequentially. A higher frequency range of interest also requires a higher spatial resolution, which may become impractical for certain applications. Sometimes, the control performance is degraded due to difficulties of installing microphones at certain locations. Furthermore, presence of physical transducers might perturb the sound field itself. For these reasons, non-intrusive, large-scale, high spatial resolution sound field measurement techniques are worthy of investigation.

Refracto-vibrometry, based on the acousto-optic effect, can serve as an excellent potential alternative [1]. Sound waves are compressional oscillatory disturbances that propagate in a fluid medium, such as air, as discussed in this article. The pressure and the density of the air are modulated with the resulting refractive index altering the light propagation, specifically regarding its amplitude and phase. These changes can be readily detected by a laser Doppler vibrometer (LDV) [1], which is sensitive to path length fluctuations. Typically, these fluctuations are caused by surface vibrations at a point on a target

of interest, thus leading to LDVs to be used to study the dynamic behaviour of materials and structures, including applications in acoustics [2, 3, 4] and, recently, to control vibration or sound [5, 6]. When the reflecting surface is stationary, the highly sensitive measurement from the LDV only results from the variations in the optical path of the fluctuating sound field, so refracto-vibrometry can be used as an alternative to reconstruct a sound field.

Early work on refracto-vibrometry first demonstrated its potential for measuring ultrasound in water [7, 8] and in air [9, 10]. More recently, studies extended the applications to the audible frequency range in air [11]. Several extensive studies have attempted to reconstruct the sound field close to a loudspeaker [12, 13]. In addition, the technique has also been used to visualise sound reflection and interference [14] and sound fields in rooms [15]. The work herein focuses on using refracto-vibrometry to measure/reconstruct the sound field at the opening of an enclosure, which might represents an aperture such as an open window. In such locations, the sound field can be complicated and thus require a large number of microphones for either sound measurement or control. It is also necessary that minimal obstructions are present for such an opening [16, 17]. This paper explores using refracto-vibrometry in this case and the quality of the reconstructed sound field will be examined in what follows and compared with that from a microphone array.

2. Refracto-vibrometry fundamentals

2.1 Measurement principle

The pressure fluctuation of a sound field changes the refractive index of the medium. In air, the refractive index, n, is proportional to the sound pressure, p, with the following relationship [12],

$$n(t) = (n_0 - 1)\left(1 + \frac{p(t)}{p_0}\right)^{\frac{1}{\gamma}} + 1 \approx n_0 + \frac{n_0 - 1}{\gamma p_0} p(t), \tag{1}$$

where n_0 is the refractive index of air under the standard atmospheric pressure, p_0 is the static atmospheric pressure, γ is the specific heat capacity ratio of air.

The phase, ϕ, of light travelling through the sound field has the following relationship with the refractive index, n

$$\phi(t) = k_0 \int_L n(t)\, dl, \tag{2}$$

where k_0 is the wavenumber of light *in vacuo* and L is the travelling path of the light. Combining Eq. (1) into (2), ϕ can be re-written as

$$\phi(t) = k_0 n_0 L + k_0 \frac{n_0 - 1}{\gamma p_0} \int_L p(l, t)\, dl = \phi_0 + \phi_p(t), \tag{3}$$

where ϕ_0 is the static phase and ϕ_p is the dynamic phase due to the sound wave. Any variation of the pressure along the path alters the measured scattering light. An LDV velocity measurement, v, is proportional to the time derivative of the phase of the light,

$$v(t) = \frac{1}{k_0 n_0} \frac{d\phi(t)}{dt}. \tag{4}$$

When an LDV is used for a vibrating object, the vibration of the surface is typically much more significant than that from the surrounding sound field, i.e., $\phi_0 \gg \phi_p$. However, when the object is stationary and not

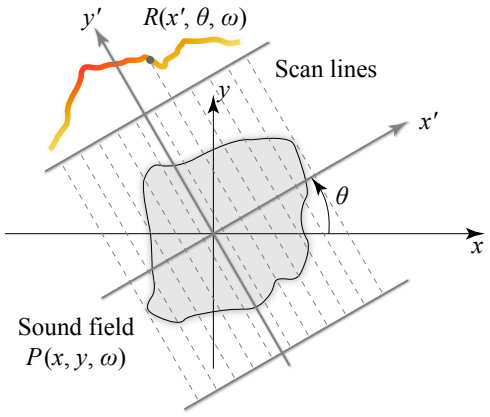

Figure 1: Demonstration of the Radon transform and parallel scan lines.

susceptible to vibration, the velocity measurement from the LDV is totally contributed by the dynamic phase, that is, the pressure fluctuation along the travelling path of the light. Therefore, Eq. (4) becomes

$$v(t) = \frac{1}{k_0 n_0}\frac{d\phi_p(t)}{dt} = \frac{n_0 - 1}{\gamma p_0 n_0}\int_L \frac{dp(l,t)}{dt}\, dl. \tag{5}$$

which, in the frequency domain, is written as

$$V(\omega) = \mathrm{i}\omega\frac{n_0 - 1}{\gamma p_0 n_0}\int_L P(l,\omega)\, dl, \tag{6}$$

with ω being the angular frequency of interest.

2.2 Radon transform

Equation (6) shows that the velocity measurements from the LDV due to the sound field are the line integrals of the optical paths rather than discrete point measurements. Such measurements are the projections "slicing" through the sound field and are described as the *Radon transform* [18]. At a projection angle θ, the Radon transform R can be mathematically expressed through

$$R(x', \theta, \omega) = \int_{-L/2}^{L/2} P(x', y', \omega)\, dy', \tag{7}$$

where x' and y' are the new coordinates rotated by the angle of θ. The demonstration of the Radon transform and the projections is shown in Fig. 1. Eq. (6) can be represented by the Radon transform as

$$V(x', \theta, \omega) = \mathrm{i}\omega\frac{n_0 - 1}{\gamma p_0 n_0} R(x', \theta, \omega), \tag{8}$$

where the velocity measurements from the LDV are the scaled Radon transform of the sound field.

3. Sound field reconstruction methods

Since the velocity measurements from the LDV are forward projections of the sound field, and are also equivalent to the Radon transform of the sound field, sound information at points within the sound field can be recovered by solving its inverse. There are various methods to achieve this as follows.

3.1 Filtered back-projection (FBP)

The FBP is the most popular and basic method of finding the inverse Radon transform. Since the measurements are the forward projections, the original sound field can be theoretically back-projected [18, 19]. The FBP method can be written as

$$P(x, y, \omega) = \frac{1}{\mathrm{i}\omega} \frac{\gamma p_0 n_0}{n_0 - 1} \int_0^{2\pi} R(x', \theta, \omega) H(\omega)\, d\theta, \tag{9}$$

where $H(\omega)$ is typically a ramp (highpass) filter to prevent oversampling at certain locations. This method essentially integrates (sums) all the projections with an adjusting filter.

3.2 Algebraic methods

Alternatively, the Radon transform can be represented algebraically as [20]

$$\mathbf{v} = \mathbf{A}\mathbf{p}, \tag{10}$$

where $\mathbf{v} \in \mathbb{C}^{JN}$ is the vector of all the velocity measurements, $\mathbf{A} \in \mathbb{C}^{JN \times MM}$ is the matrix representing the (discrete) Radon transform, and $\mathbf{p} \in \mathbb{C}^{MM}$ is the vector of the sound pressure of all the points in the sound field. It is assumed that there are N light beams per projection angle and that there are J angles. There are $M \times M$ points to be determined in the sound field, which defines an inverse problem. Once the system is identified, that is, $\mathbf{A}$ is modelled, the sound pressure of all the points within the sound field can be found.

3.2.1 Truncated singular value decomposition (TSVD)

When $\mathbf{A}$ is written in the form of SVD, i.e.,

$$\mathbf{A} = \mathbf{U}\mathbf{\Sigma}\mathbf{V}^H, \tag{11}$$

where $\mathbf{U} \in \mathbb{C}^{JN \times JN}$ and $\mathbf{V} \in \mathbb{C}^{MM \times MM}$ are orthogonal matrices. $\mathbf{\Sigma} \in \mathbb{C}^{JN \times MM} = \mathrm{diag}(\sigma_1, \sigma_2, \ldots, \sigma_r)$ is a diagonal matrix with the singular values of $\mathbf{A}$. The solution can be found by [21]

$$\mathbf{p} = \mathbf{A}^\dagger \mathbf{v} = \mathbf{V}\mathbf{\Sigma}^\dagger \mathbf{U}^H \mathbf{v}, \tag{12}$$

where $\mathbf{\Sigma}^\dagger = \mathrm{diag}(1/\sigma_1, 1/\sigma_2, \ldots, 1/\sigma_{r_\alpha}, 0, \ldots, 0),\ (r_\alpha < r)$. The † symbol denotes pseudoinverse. Certain small singular values are truncated to prevent unstable inverse results.

3.2.2 Tikhonov regularisation

The Tikhonov regularised solution [22, 23] of Eq. (10) can be found through

$$\mathbf{p} = \mathrm{argmin} \left\{ \|\mathbf{A}\mathbf{p} - \mathbf{v}\|_2^2 + \lambda \|\mathbf{p}\|_2^2 \right\}, \tag{13}$$

where λ is the regularisation parameter. The solution to the Tikhonov regularised optimisation problem is

$$\mathbf{p} = (\mathbf{A}^H \mathbf{A} + \lambda \mathbf{I})^{-1} \mathbf{A}^H \mathbf{v}, \tag{14}$$

where superscript ^{H} denotes Hermitian transpose, $\mathbf{I}$ is the identity matrix.

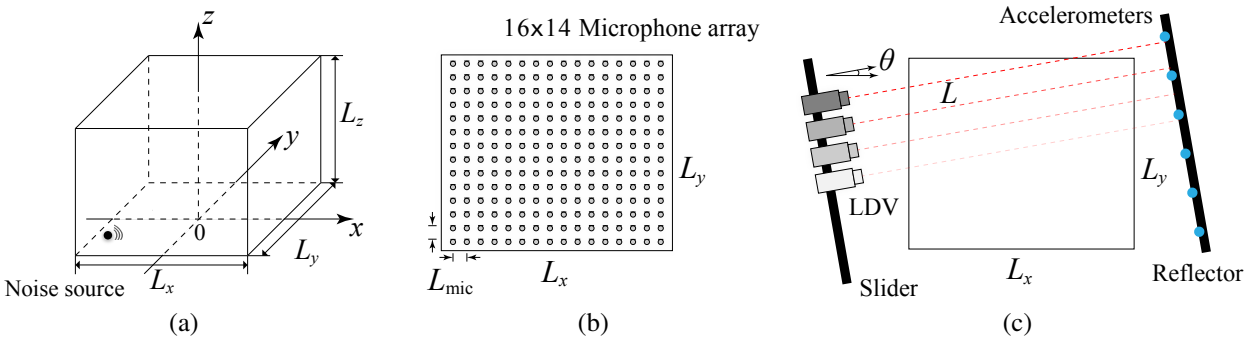

Figure 2: (a) The coordinate and s of the enclosure under investigation. The opening is at the topside. (b) Configuration of the 16×14 microphone array to measure the sound field at $z = 0.95$ m. (c) Sound field measurement/reconstruction by refracto-vibrometry using an LDV on a motorised slider. The optical path has a length of L, and the projection angle is θ.

4. Experiments

4.1 System setup

The sound field under investigation was at an opening of an enclosure as shown in Fig. 2a. The opening was at the topside. The enclosure had dimensions of $(L_x \times L_y \times L_z) = (1 \times 0.85 \times 0.9)$ m and was made from acrylic material with 10 mm thickness. A sound source (a Genelec 8010A studio monitor) was placed at the coordinate $(-0.4, -0.4, 0.1)$ m coordinate. The sound field to be measured was located at the $z = 0.95$ m plane. Figure 2b shows the traditional sound field measurement using a 16×14 microphone array (Brüel & Kjær Type 4957) with $L_{\text{mic}} = 60$ mm spacing. Figure 2c shows the setup of using the refracto-vibrometry with an LDV to reconstruct the sound field. The LDV (Polytec PDV-100) was mounted on a 1.5 m motorised ball-screw slider actuated by a stepper motor (NEMA23). The reflector was a steel beam was located $L = 1.5$ m away across the field with retro-reflective tape adhered for the maximum laser beam reflection. Accelerometers (Brüel & Kjær Type 4533-B) were adhered to the reflector at six spots close to the laser reflection spots to monitor the vibration of the reflector. There were 131 scan lines per projection angle with an invterval of 10 mm and 36 projection angles, i.e., $\theta \in [0 : 10 : 350]$. All signals were acquired and recorded through the Brüel & Kjær DAQ modules (Type 3053 and 3160) and the sampling rate was set to 131.072 kHz. The atmospheric condition was measured through a thermo-hygro-barometer (RS-1160). The heat ratio of air was $\gamma = 1.4$, the static pressure was $p_0 = 101.32$ kPa, the room temperature was 25.0 °C and the relative humidity was measured to be 47.6 %. The static refractive index of air n_0 was hence calculated to be 1.0002667951 [14].

4.2 Results

4.2.1 Measurement validation

By comparing the measurements from both the LDV and the accelerometers, which are shown in Fig. 3, it is validated that the velocity measurements from the LDV are caused by the acousto-optic effect. From the six spots on the reflector, it is clear that the acousto-optic effect is prominent generally above 500 Hz. Below 500 Hz, the reflector can be easily acoustically excited and is thus not suitable for the refracto-vibrometry technique at lower frequencies. Future work is planned to further validate the LDV measurements including the effect of the stand-off distance (relative to the reflector) and the laser measurement location (currently on the reflector surface).

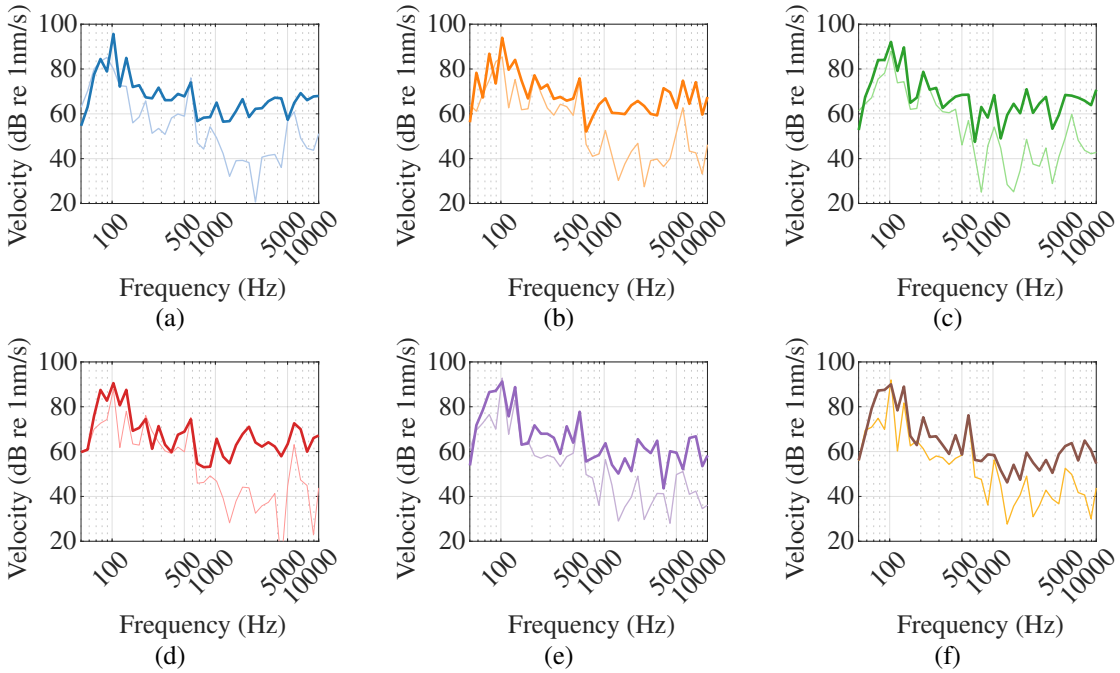

Figure 3: Velocity measurements (thick lines) from the LDV across the sound field and from the accelerometers (thin lines) adhered to the rigid reflector at six locations.

4.2.2 Sound field reconstruction

The specific tonal frequency under investigation is 500 Hz. Figure 4 shows the sound pressure levels (SPLs) measured by the microphone array as the reference (a), whereas the reconstructed sound fields from the aforementioned three methods – (b) FBP, (c) TSVD and (d) Tikhonov – are compared.

The reconstructed sound field from the FBP method as shown in Fig. 4b is the least satisfactory among the three techniques. Although the general form is similar to the reference case, "lumpy" artefacts can occur with this method when the measurements are noisy and/or the amount of data is sub-optimal. In addition, the only adjustable parameter is the highpass filter, which makes it the least favourable for sound field reconstruction. The result from the TSVD is shown in Fig. 4c. Here, the singular values in Eq. (12) have been truncated to $r_\alpha = 800$ from a total of 4,716. Similar artefacts in Fig. 4b are still present, though they are improved compared to those from the FBP method. The best result among the three techniques is that from the Tikhonov regularisation method ($\lambda = 1 \times 10^{-7}$ in Eq. (14)). The overall reconstructed sound field is the smoothest and is the closest to the one measured by the 16×14 microphone array. Further work may improve these new findings and is certainly required to more quantitatively compare and contrast them against the microphone array result.

5. Conclusions

In this study, three methods, namely the filtered back-projection, the truncated singular value decomposition and the Tikhonov regularisation methods, have been used to evaluate the sound field at the opening of an enclosure from a laser Doppler vibrometer based refracto-vibrometry measurement campaign. Using the measurement from a microphone array as the reference, the Tikhonov regularisation method yields the best result, whereas the filtered back-projection method gives the least satisfactory result. Further work includes investigating the impact on the result of differences in the underlying LDV measurements and comparing them quantitatively with that from the microphone array. In the future,

LDV-based refracto-vibrometry can potentially be used in in this way for a variety of sound field control applications where the introduction of microphone array is practically challenging or commercially prohibitive.

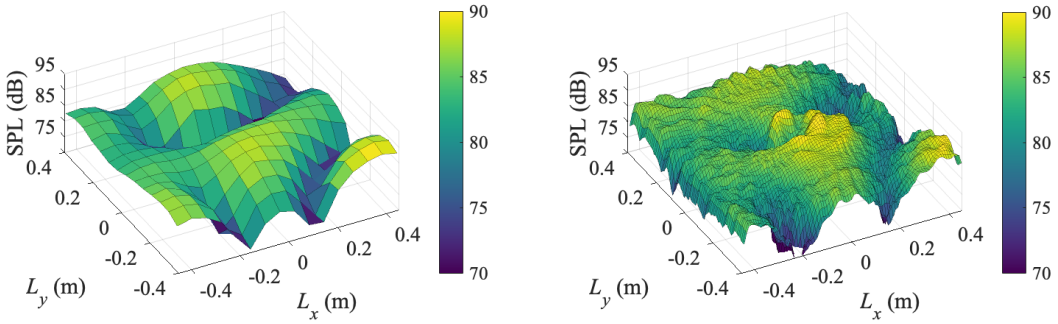

(a) Microphone array

(b) FBP

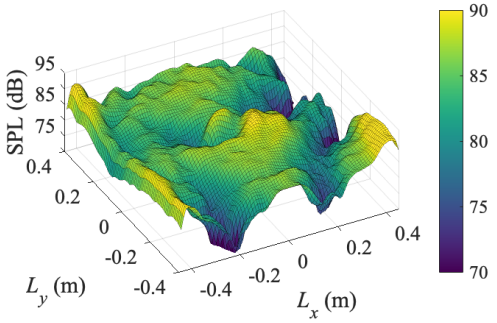

(c) TSVD

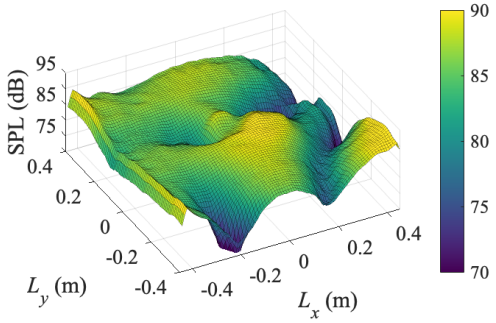

(d) Tikhonov

Figure 4: The SPLs measured by the 16×14 microphone array and reconstructed from the FBP, the TSVD and the Tikhonov regularisation methods.

REFERENCES

1. Rothberg, S., et al. An international review of laser doppler vibrometry: Making light work of vibration measurement, *Optics and Lasers in Engineering*, **99**, 11–22, (2017).

2. Bissinger, G. and Oliver, D. 3-d laser vibrometry on legendary old italian violins, *Sound and Vibration*, **41** (7), 10–15, (2007).

3. Suh, J.-G., Cho, W.-H., Kim, H.-Y., Cui, Z. and Suzuki, Y. Sensitivity measurement of a laboratory standard microphone by measuring the diaphragm vibration, *Applied Acoustics*, **143**, 38–47, (2019).

4. Xiao, T., Zhao, S., Qiu, X. and Halkon, B. Using a retro-reflective membrane and laser doppler vibrometer for real-time remote acoustic sensing and control, *Sensors*, **21** (11), (2021).

5. Wang, T., Li, R., Zhu, Z. and Qu, Y. Active stereo vision for improving long range hearing using a laser doppler vibrometer, *2011 IEEE Workshop on Applications of Computer Vision (WACV)*, pp. 564–569, IEEE, (2011).

6. Xiao, T., Qiu, X. and Halkon, B. Ultra-broadband local active noise control with remote acoustic sensing, *Scientific reports*, **10** (1), 1–12, (2020).

7. Pitts, T. A. and Greenleaf, J. F. Three-dimensional optical measurement of instantaneous pressure, *The Journal of the Acoustical Society of America*, **108** (6), 2873–2883, (2000).

8. Harland, A. R., Petzing, J. N. and Tyrer, J. R. Nonperturbing measurements of spatially distributed underwater acoustic fields using a scanning laser doppler vibrometer, *The Journal of the Acoustical Society of America*, **115** (1), 187–195, (2004).

9. Nakamura, K., Hirayama, M. and Ueha, S. Measurements of air-borne ultrasound by detecting the modulation in optical refractive index of air, *2002 IEEE Ultrasonics Symposium, 2002. Proceedings.*, vol. 1, pp. 609–612, IEEE, (2002).

10. Zipser, L., Franke, H., Olsson, E., Molin, N.-E. and Sjödahl, M. Reconstructing two-dimensional acoustic object fields by use of digital phase conjugation of scanning laser vibrometry recordings, *Appl. Opt.*, **42** (29), 5831–5838, (2003).

11. Oikawa, Y., Goto, M., Ikeda, Y., Takizawa, T. and Yamasaki, Y. Sound field measurements based on reconstruction from laser projections, *Proceedings.(ICASSP'05). IEEE International Conference on Acoustics, Speech, and Signal Processing, 2005.*, vol. 4, pp. iv–661, IEEE, (2005).

12. Torras-Rosell, A., Barrera-Figueroa, S. and Jacobsen, F. Sound field reconstruction using acousto-optic tomography, *The Journal of the Acoustical Society of America*, **131** (5), 3786–3793, (2012).

13. Yatabe, K., Ishikawa, K. and Oikawa, Y. Acousto-optic back-projection: Physical-model-based sound field reconstruction from optical projections, *Journal of Sound and Vibration*, **394**, 171–184, (2017).

14. Malkin, R., Todd, T. and Robert, D. A simple method for quantitative imaging of 2d acoustic fields using refracto-vibrometry, *Journal of Sound and Vibration*, **333** (19), 4473–4482, (2014).

15. Verburg, S. A. and Fernandez-Grande, E. Acousto-optical volumetric sensing of acoustic fields, *Physical Review Applied*, **16** (4), 044033, (2021).

16. Qiu, X., *An Introduction to Virtual Sound Barriers*, CRC Press (2019).

17. Wang, S., Tao, J., Qiu, X. and Pan, J. A boundary error sensing arrangement for virtual sound barriers to reduce noise radiation through openings, *The Journal of the Acoustical Society of America*, **145** (6), 3695–3702, (2019).

18. Kak, A. C. and Slaney, M., *Principles of computerized tomographic imaging*, SIAM (2001).

19. Barrett, H. H. Iii the radon transform and its applications, *Progress in optics*, **21**, 217–286, (1984).

20. Bertero, M. and Boccacci, P., *Introduction to inverse problems in imaging*, CRC press (2020).

21. Hansen, P. C. Truncated singular value decomposition solutions to discrete ill-posed problems with ill-determined numerical rank, *SIAM Journal on Scientific and Statistical Computing*, **11** (3), 503–518, (1990).

22. Tikhonov, A. N. and Arsenin, V. Y. Solutions of ill-posed problems, *New York*, **1**, 30, (1977).

23. Oberst, S., Nava-Baro, E., Lai, J. C. and Evans, T. A. An innovative signal processing method to extract ants' walking signals, *Acoustics Australia*, **43** (1), 87–96, (2015).